*Desalination and Water Treatment*
www.deswater.com

doi: 10.1080/19443994.2015.1041161

57 (2016) 10333–10348
May

Taylor & Francis
Taylor & Francis Group

# Surface modification of electrospun PAN nanofibers by amine compounds for adsorption of anionic dyes

A. Almasian[a,*], Gh. Chizari Fard[b], M. Parvinzadeh Gashti[c], M. Mirjalili[c], Z. Mokhtari Shourijeh[d]

[a]*Department of Environmental Research, Institute for Color Science and Technology, Tehran, Iran, email: almasian-ar@icrc.ac.ir*
[b]*Department of Textile, Islamic Azad University, Yazd Branch, Yazd, Iran, email: chizarifard@iauyazd.ac.ir*
[c]*Department of Textile, Islamic Azad University, Shahre Rey Branch, Tehran, Iran, emails: parvinzadeh@gmail.com (M. Parvinzadeh Gashti), Dr.mirjalili@iauyazd.ac.ir (M. Mirjalili)*
[d]*Young Researcher, Islamic Azad University, South Tehran Branch, Tehran, Iran*

Received 2 November 2014; Accepted 20 March 2015

ABSTRACT

Within the present study, polyacrylonitrile (PAN) nanofibers were produced by electrospinning technique. The surface of the webs was then modified by three different sources of amine-containing compounds, including diethylamine, diethylenetriamine, and triethylenetetramine. Chemical, morphological, and surface properties of nanofibers were investigated by attenuated total internal reflection (ATR) spectroscopy, scanning electron microscopy (SEM), and atomic force microscopy (AFM), respectively. The maximum grafting yield of amine groups to PAN nanofibers was calculated by the gravimetric method. The ATR results indicated that amide groups were formed on the fiber surface by a chemical reaction between the nitrile groups of PAN and the amine groups of amine-containing compounds. The SEM images showed a rough, conglutinated, and intertwined surface morphology of nanofibers induced by amine-containing materials. The AFM results showed that after the functionalization process, the surfaces of the PAN nanofiber were rougher when compared with untreated PAN nanofiber. Finally, their dye removal ability was evaluated using UV–vis spectroscopy using Direct red 80 (DR80) and Direct red 23 (DR23) as model compounds. The amounts of the dye adsorbed onto the functionalized PAN nanofibers (FPAN) were influenced by the initial pH, FPAN dosage, contact time, and the initial concentration of the dye solutions. It was found that both dyes adsorption followed the Langmuir isotherm. In addition, adsorption kinetics of both dyes was found to conform to pseudo-second-order kinetics. We finally found that the functionalized PAN nanofibers were good candidates for anionic dye adsorption from colored wastewater with high dye adsorption capacity

*Keywords:* Polyacrylonitrile (PAN); Electrospinning; Diethylamine; Diethylenetriamine; Triethylenetetramine; Surface modification; Direct red 80; Direct red 23; Adsorption isotherm; Dye kinetic

*Corresponding author.

## 1. Introduction

Industrial wastewaters have been recognized as one of the largest sources of water contamination. Discharge of pollutants with a variety of organic compounds and toxic substances is harmful to human and aquatic life [1–7]. Among the various industries, textile production consumes large quantities of water in different steps and there are restricted roles to inhibit discharging of highly colored wastewaters from dyeing houses [8,9]. As a result, the removal of dyes from waste effluents has become environmentally critical. Among several methods, the adsorption process has been recognized as one of the most effective techniques for dye removal from wastewater. Many adsorbents are introduced including activated carbon, perlite, soybean hull, sawdust, kaolinite clay, and rice straw [10]. However, they suffer from some limitations such as poor heat, mechanical resistance, and relatively low adsorption capacity for pollutants [11]. Polymeric adsorbents have been increasingly used for dye removal due to their wide variation in surface chemistry, regenerability on site, and porosity [12]. The adsorption capacity of adsorbents can be improved by introducing various functional groups (carboxyl, tetrazine, sulfonic, amino, and phosphoric groups) on the surface with selective adsorption affinity to targeted adsorbates [13–16]. Among them, amine-functionalized adsorbents are highly considered because of their ability in formation of strong complexes with pollutants [17,18].

Polyacrylonitrile (PAN) is known as an environmental stable polymer that can be easily electrospun into nanofibers. Recently, many studies have been conducted on PAN surface modification for adsorption of heavy metal ions [19–21]. Among them, ethylenediamine and diethylenetriamine compounds are widely used. However, there is no report on investigation of dye removal ability of PAN nanofibers modified by amine-containing compounds.

In this study, the surface of electrospun PAN nanofibers was chemically modified by amine-containing compounds of diethylamine, diethylenetriamine, and triethylenetetramine. The anionic dye adsorption of resultant nanofibers was studied by considering several parameters including contact time, adsorbent amount, dye concentration, and solution pH. Furthermore, the equilibrium data were analyzed using various adsorption isotherms.

## 2. Experimental section

### 2.1. Materials

Polyacrylonitrile copolymer (93.7% acrylonitrile and 6.3% vinylacetate with $M_w$ = 100.000 g/mol) was purchased from Isfahan Polyacryl Inc. (Iran). N,N-dimethylformamide (DMF), potassium carbonate, diethylamine (DEA, hereafter), diethylenetriamine (DETA, hereafter), and triethylenetetramine (TETA, hereafter) were used as received from Merck. DR80 was supplied by AlvanSabet Co. Iran. The chemical structures of the dyes are shown in Fig. 1.

### 2.2. Electrospinning of PAN nanofibers

Electrospinning solution was prepared by 10 w/w% PAN copolymer dissolved in DMF. Mechanical stirring was applied for 12 h at room temperature in order to obtain homogeneous PAN solution. The as-prepared solution was then electrospun under a fixed electric field of 17 kV using a Gamma High Voltage Research RR60power supply onto aluminum (Al) sheet which was used as the collector. The distance from the tip to the collector was 16 cm and the feeding rate of the polymer solution was 1.2 mL/h. The electrospun nanofibers mat was placed at a vacuum oven (75˚C, 8 h) to ensure evaporation of the solvent.

### 2.3. Preparation of surface-functionalized PAN nanofibers

The functionalized PAN nanofibers (hereafter, FPAN) were synthesized by immersing nanofibers in a mixture of an amine-containing compound (16.5 mL), potassium carbonate (catalyst; 1 g), and distilled water (33.5 mL) in a 250-mL beaker connected to a reflux column. The reactions for diethylamine (hereafter, FPAN1), diethylenetriamine (hereafter, FPAN2), and triethylenetetramine (hereafter, FPAN3) compounds were carried out at 95˚C for 6, 3, and 2 h, respectively. The nanofibers were then separated from the solution, rinsed with distilled water up to a near neutral pH value, and finally dried at 80˚C in an oven overnight.

### 2.4. Characterization

The ATR spectra of untreated PAN and various FPAN nanofibers were examined by the ATR spectroscopy (ThermoNicolet NEXUS 870 FTIR from Nicolet Instrument Corp., USA). The surface morphology and topography of all electrospun nanofibers were investigated using a scanning electron microscope (SEM, LEO1455VP, ENGLAND) and atomic force microscope (AFM, DualScope C-26, DENMARK), respectively.

The conversion of nitrile groups into amidine groups ($C_n$ %) on the surface of each FPAN nanofiber was calculated by gravimetry and estimated based on the following equation [22]:

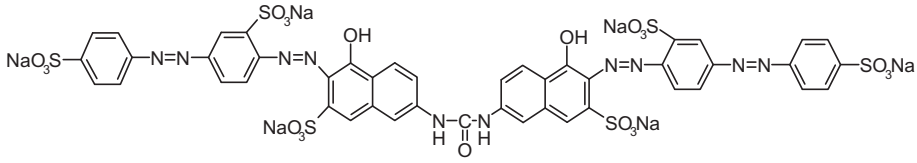

Direct Red 80

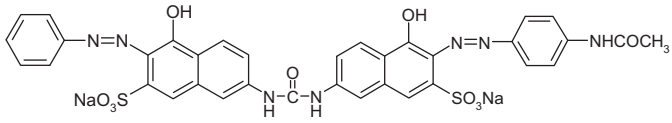

Direct Red 23

Fig. 1. The chemical structure of dyes.

$$C_n = \frac{W_1 - W_0}{W_0} * \frac{M_0}{M_1} * 100 \quad (1)$$

where $W_1$ and $W_0$ are the weights of the PAN nanofibers after and before the reaction, respectively; $M_0$ is the molecular weight of the acrylonitrile monomer (i.e., 53 g mol$^{-1}$), and $M_1$ is the molecular weight of each amine compounds (DEA = 73.14, DETA = 103.17, TETA = 146.23 g mol$^{-1}$).

Surface chemical characterization was performed by X-ray photoelectron spectroscopy (XPS) using a Thermo ESCALAB 280 system with Al/Kα ($hv$ = 1,486.6 eV) anode mono X-ray source.

A known weight of the nanofiber is decomposed by digestion with concentrated sulfuric acid, preferably in the presence of a catalyst (e.g. a mixture of selenium, copper sulfate, and potassium sulfate) to accelerate the process; ammonium sulfate is produced. An excess of sodium hydroxide solution is added to the diluted reaction mixture, and the ammonia is distilled in steam, and absorbed in excess of 0.04 N hydrochloric or sulfuric acid. Titration of the residual mineral acid with 0.04 N sodium hydroxide gives the equivalent of the ammonia obtained from the weight of sample taken. The percentage of nitrogen can be easily calculated.

Calculate the percentage of nitrogen in the nanofiber from the following formula:

$$\text{Percentage of nitrogen} = \frac{100 * (V_1 - V_2) * 0.5603}{W} \quad (2)$$

where $V_1$ = volume (ml) of 0.04 N hydrochloric acid consumed in the determination, $V_2$ = volume (ml) of 0.04 N hydrochloric acid consumed in the blank, and $W$ = weight (mg) of nanofiber taken.

### 2.5. Adsorption studies

Different FPAN nanofibers specimens were individually placed in a batch containing 30, 70, 250 mL solution of DR80 and DR23 with a concentration of 40 mg/L to evaluate the adsorption capacity of FPAN1, FPAN2, and FPAN3, respectively. The pH of each solution was adjusted to a desired value using HCl or NaOH solution. Single—beam UV spectrophotometer (CECIL CE2021) is used for adsorption measurements. The amounts of decolorization from solutions were determined as a function of time according to the following equation:

$$\text{Dec } \% = \frac{A_0 - A}{A_0} \times 100 \quad (3)$$

where $A_0$ and $A$ are dye concentrations at $t$ = 0 and $t$, respectively.

The effect of adsorbent dosage on the dye removal was studied by contacting 30, 70, 250 mL of each dye solution (for FPAN1, FPAN2, and FPAN3, respectively) with initial concentration of 40 mg/L and pH 2.1 at room temperature for 60 min with adsorbents. Different amounts of nanofibers were applied to remove DR80 and DR23.

The effect of pH on the dye removal was investigated by contacting 30, 70, 250 mL of dye solution with nanofibers (i.e. 0.007, 0.003, and 0.003 g for FPAN1, FPAN2, and FPAN3, respectively) and initial dye concentration (40 mg/L) at room temperature for

60 min. Different pH values (2.1, 6.5, and 9.1) were used to remove dyes.

Finally, the effect of the initial dye concentration on the dye removal was investigated by contacting 30, 70, 250 mL of the dye solution with nanofibers (i.e. 0.007, 0.003, and 0.003 g for FPAN1, FPAN2, and FPAN3, respectively) at pH 2.1 and room temperature for 60 min. Different initial dye concentrations (40, 60, 80, and 100 mg/L) were applied to remove dyes.

## 3. Results and discussion

### 3.1. ATR-FTIR of various PAN nanofibers

The ATR spectra of the untreated PAN and various FPAN nanofibers are shown in Fig. 2. The untreated PAN spectrum (curve a) exhibited the absorption peaks of stretching vibrations for OH groups at 3,542 $cm^{-1}$, C ≡ N and at 2,244 $cm^{-1}$, C=O bond at 1,741 $cm^{-1}$ [23,24], CH stretching in CH, $CH_2$, and $CH_3$ groups at 2,941 $cm^{-1}$ [24,25], and C–O groups at 1,200–300 $cm^{-1}$ [26]. These assignments suggest that PAN is a copolymer containing both acrylonitrile and vinylacetate polymers. In the spectra of the FPAN nanofibers, the band intensity at 3,445 $cm^{-1}$ corresponding to overlapping of the stretching vibration bands of OH and NH groups increased and shifted to the lower wave numbers from 3,542 to 3,445 $cm^{-1}$ compared to the untreated PAN. It can be concluded that many OH and NH groups were introduced or formed on the surface of FPAN nanofibers by the hydrolysis of ester groups in PAN and immobilization of amine compounds. Such a result is further supported by decreasing in the intensity of the band at 1,726 (relating to C=O bond) $cm^{-1}$ (for FPAN1) and disappearance of the band (at 1,726 $cm^{-1}$) for FPAN2 and FPAN3nanofibers confirming hydrolysis of the acetate ester groups. In the spectra of FPAN nanofibers, the presence of new absorption band at 1,560 $cm^{-1}$, and shifting of a band from 1,629 to 1,665 $cm^{-1}$ can be assigned to the bending vibrations of secondary amines and the stretching vibrations of amidine group (N–C=N), respectively. The intensity of a peak associated with nitrile groups at 2,244 $cm^{-1}$ also decreased for FPAN1 nanofibers, and disappeared for FPAN2 and FPAN3nanofibers. These changes indicate the reaction between nitrile groups of PAN copolymer and amine groups of amine compounds. With regard to Fig. 2, it is further obvious that the intensity of a band at 1,665 $cm^{-1}$ (amidine group) was increased when the number of amine group increased in samples modified with amine-containing compounds. It can be concluded that the number of converted nitrile group to amidine group was increased with increasing the number of amine groups in amine compound. Furthermore, it is worth mentioning that the number of nitrile groups on the surface of FPAN nanofibers modified with DETA and TETA compounds were too low by the reason of high conversion amount of nitrile to amidine groups and difficult for detection by ATR spectrophotometer.

### 3.2. Morphology of various surface-modified PAN nanofibers

Fig. 3 shows SEM images of untreated PAN and different PAN nanofibers modified by amine-containing compounds. As it can be seen, the surface of all FPAN nanofibers became rougher than the untreated PAN nanofiber. FPAN3 showed the roughest surface among the various FPAN nanofibers. The SEM image of FPAN1 nanofibers showed some defects, cracks, and signs of degradation on the surface of nanofibers probably due to more residence time of FPAN1 nanofibers in high temperature and alkaline condition of surface grafting process. From the images, it is clear that the FPAN3 nanofibers were conglutinated to each other at touching points and became more intertwined because of stronger crosslinking role of triethylenetetramine compared with other amine-containing compounds. Furthermore, the average diameter of nanofibers increased from 230 (for untreated PAN nanofiber) to 330, 270, and 310 nm for FPAN1, FPAN2, and FPAN3, respectively, due to swelling of nanofibers after the functionalization process. It is obvious that the residence time in functionalization process had a significant effect on fiber diameter.

### 3.3. AFM analysis

Fig. 4 shows the AFM images of the untreated PAN and different FPAN nanofibers. AFM technique can give information on the changes in the surface roughness of a sorbent. The average roughness ($S_a$) of the surfaces can be calculated from the roughness profile obtained from the AFM images. For the untreated PAN, FPAN1, FPAN2, and FPAN3 nanofibers, the value of $S_a$ was 16.3, 25.3, 22.5, and 27.5 nm, respectively, which indicates that the surfaces of the PAN nanofiber became rough after the functionalization process. As it can be seen, the average roughness of FPAN1 nanofiber is higher than FPAN2 nanofiber. Furthermore, the average roughness of FPAN3 nanofiber is higher than other samples possibly due to more reactivity for the sample treated with TETA in comparison with other amine-containing compounds. It can be elucidated that surface roughness of fibers is

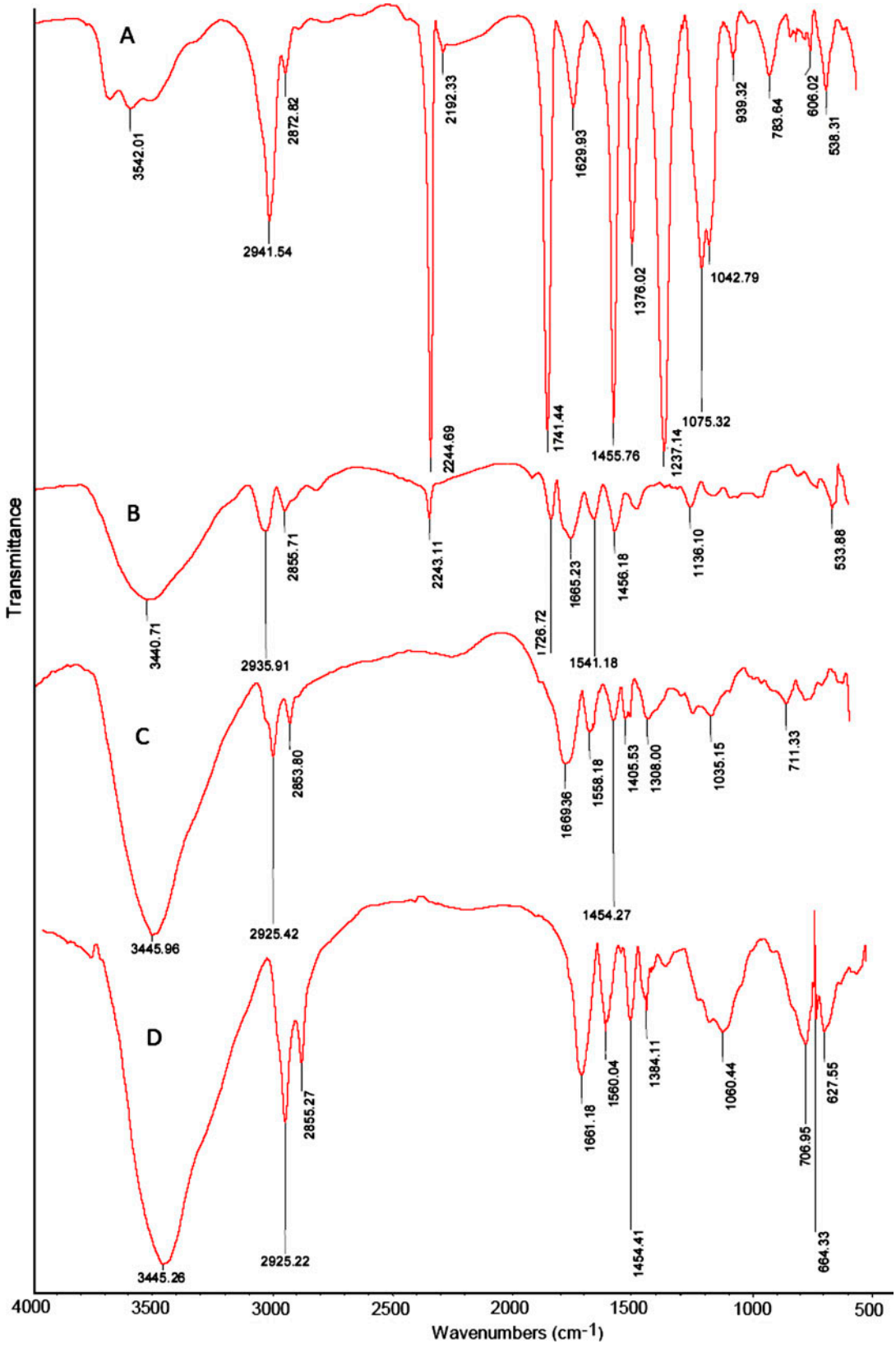


Fig. 2. ATR spectra of (A) untreated PAN nanofiber, (B) FPAN1 nanofiber, (C) FPAN2 nanofiber, and (D) FPAN3 nanofiber.

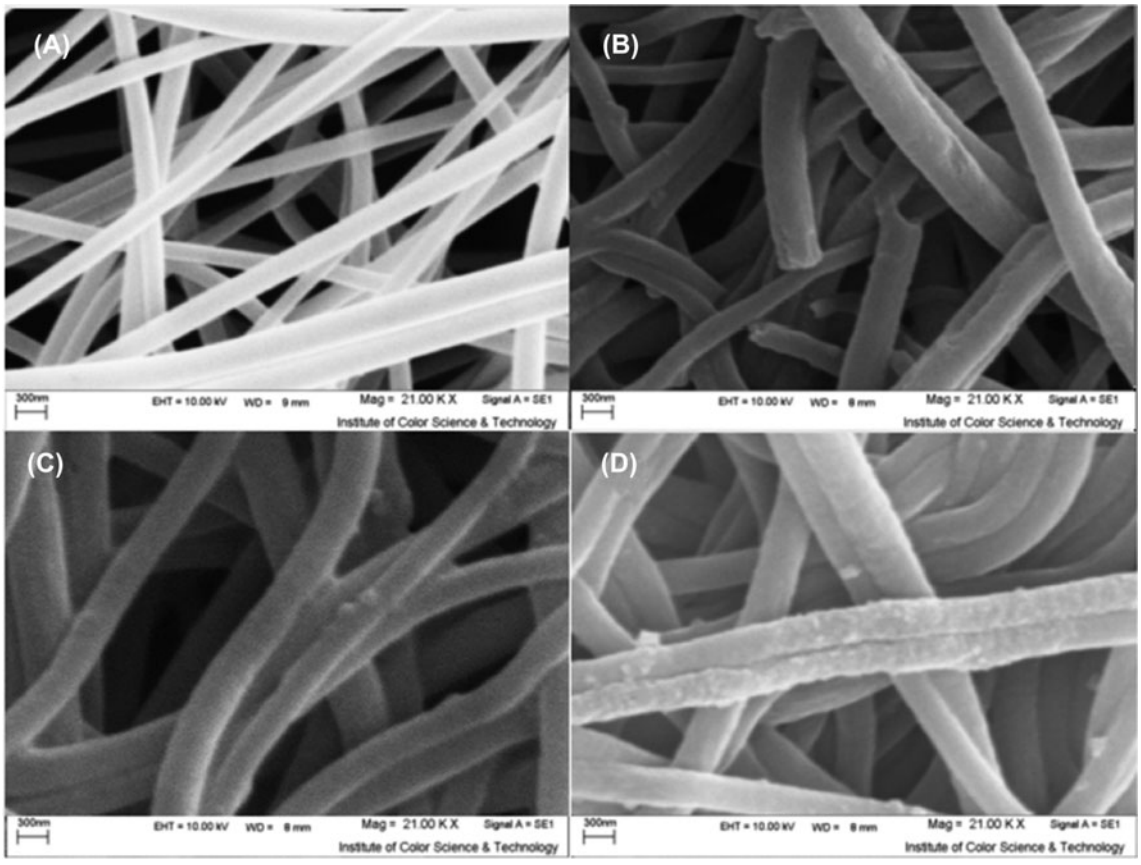


Fig. 3. SEM images of (A) untreated PAN nanofiber, (B) FPAN1 nanofiber, (C) FPAN2 nanofiber, and (D) FPAN3 nanofiber.

highly related to the reactivity of amine-containing compound and duration of process as well as the temperature. We also found that the reactivity of amine-containing compound has the most influence on the roughness of fibers.

### 3.4. Optimization of grafting conditions

In order to optimize grafting process, the time of reaction is varied to study the conversion amount of nitrile groups in PAN nanofibers ($C_n$ %). The dye removal percentage was investigated afterwards and results are shown in Fig. 5 and Table 1. As it can be seen, the amount of conversion ($C_n$ %), as well as the dye removal percentage, increased with increasing the time of reaction. The grafting time was different for different amine-containing compounds used in this study due to the variation of molecular weight. Since the boiling point of a compound has a direct relation with molecular weight, a compound with more molecular weight requires less reaction time. It is stated that the conversion amount of nitrile groups in PAN increased with increasing the temperature of reaction because of the endothermic conditions [26]. The temperature of the reaction batch was fixed at the boiling point of DEA (55.6°C), so the time required for completion of the reaction increased to 6 h. It was estimated that, the required time for grafting increases about 1 h with each 10°C decreasing from the boiling point of an amine-containing compound compared to the chosen reaction temperature (95°C). Based on our primary results, the optimum reaction time for grafting of PAN nanofibers was determined to be 6, 3, and 2 h for DEA, DETA, and TETA compounds, respectively.

The chemical composition of various nanofibers was analyzed by XPS and results are shown in Table 2. As can be seen, the percentage of nitrogen atoms detecting on the surface of nanofiber increased due to immobilization of amine group on the surface after the functionalization process. This increment was intensified when a heavier amine-containing compound was used. Moreover, the lower O/N ratio might imply a higher content of amine functional groups at the nanofiber surface. Also, the percentage of nitrogen was evaluated by KJELDAHL method [27]. From the results, it is clear that the percentage of

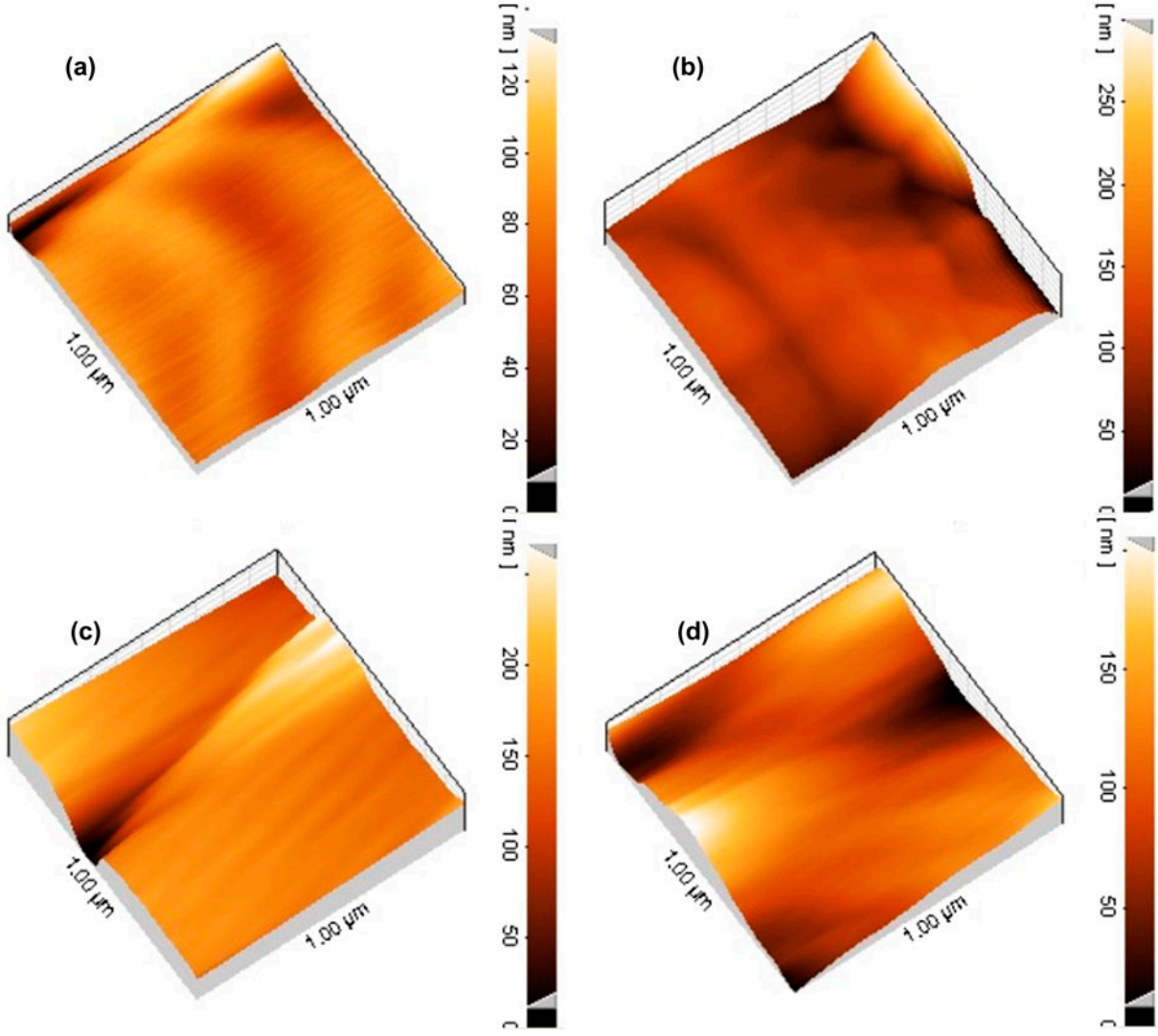


Fig. 4. AFM images of (a) untreated PAN nanofiber, (b) FPAN1 nanofiber, (c) FPAN2 nanofiber, and (d) FPAN3 nanofiber.

nitrogen increased after the functionalization process due to the incorporation and generation of amine group to the PAN polymer.

### 3.5. Adsorption studies

#### 3.5.1. Effect of adsorbent dosage

The plot of dye removal (%) versus time (min) at different FPAN nanofiber dosages (g) is shown in Fig. 6. The adsorption process for the FPAN nanofibers was found to be rapid. The amount of adsorbed dyes onto the FPAN nanofibers increased rapidly in the first 5 and 15 min for DR80 and DR23, respectively, and then slowed down reaching a constant value. This rapid adsorption is due to availability of a great number of free adsorptive sites and the high concentration of the dyes used. The decrease in the dye removal rate after the first 5 and 15 min can be attributed to the decrease in the adsorptive sites as well as the dye concentration. However, the adsorption capacity (milligrams of adsorbed dye per gram of adsorbent) decreased with increasing the amount of sorbent because of aggregation of adsorption sites. This further resulted in a decrease in total adsorbent surface area available to the dye molecules and an increase in diffusion path length [28]. High percentage of dye removal has a direct relation with the introduction of active sites on the surface of nanofibers. Based on the results, the optimum dosage of FPAN1, FPAN2, and FPAN3 nanofibers is 0.007, 0.003, and 0.003 g, respectively, for both DR80 and DR23.

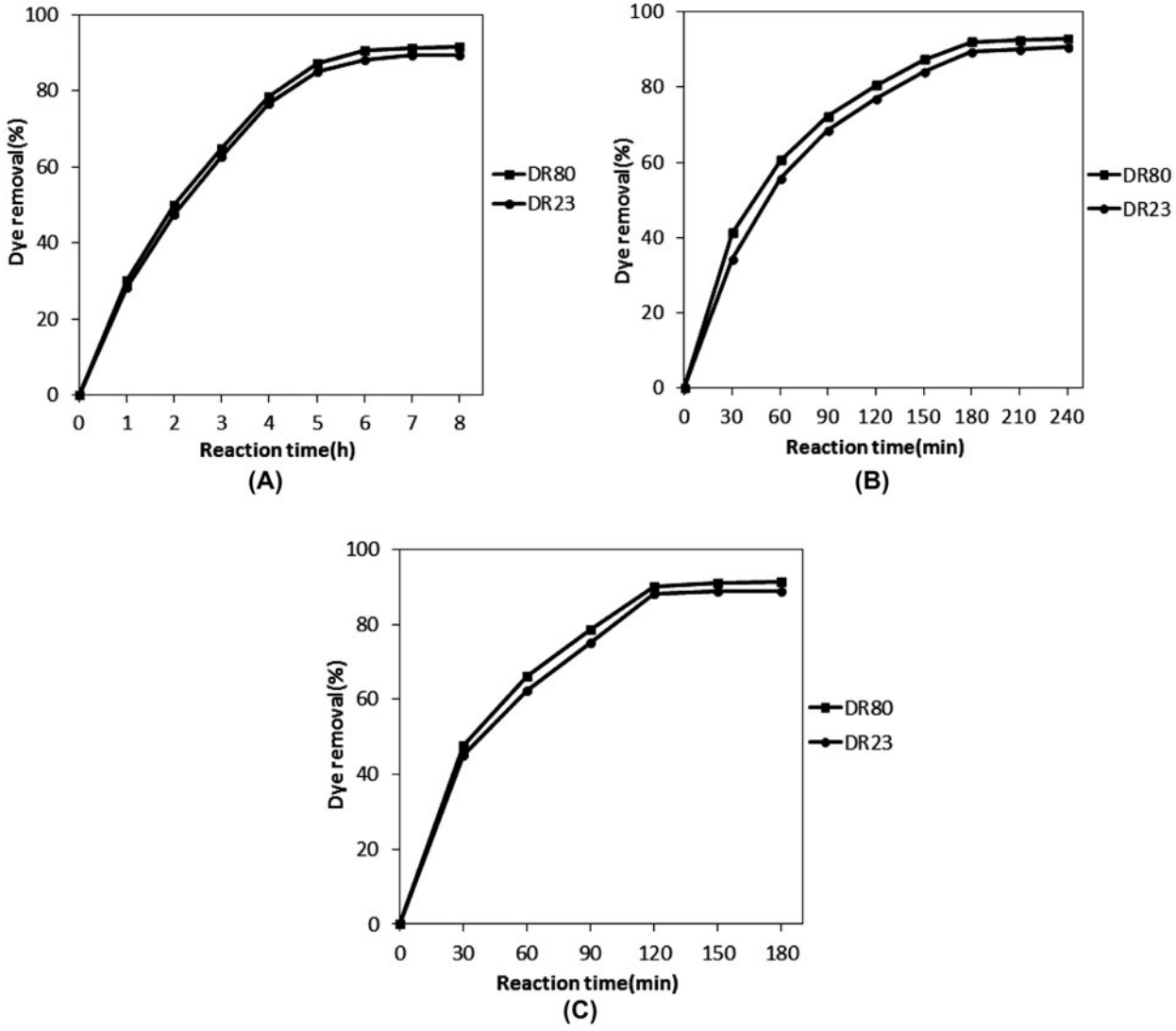


Fig. 5. Effect of grafting time on the dye removal (A) FPAN1, $V$ = 30 mL, 0.007 g, (B) FPAN2, $V$ = 70 mL, 0.003 g, and (C) FPAN3, $V$ = 250 mL, 0.003 g, at pH 2.1, 40 ppm (dye concentration).

Table 1
Conversion ($C_n$, in %) of the nitrile group of the functionalized PAN with various amine compounds

| FPAN1 | | FPAN2 | | FPAN3 | |
|---|---|---|---|---|---|
| Time (h) | $C_n$ (%) | Time (min) | $C_n$ (%) | Time (min) | $C_n$ (%) |
| 1 | 7.33 | 30 | 10.25 | 30 | 19.14 |
| 2 | 11.21 | 60 | 14.16 | 60 | 28.59 |
| 3 | 13.56 | 90 | 17.02 | 90 | 49.46 |
| 4 | 21.21 | 120 | 19.55 | 120 | 63.55 |
| 5 | 29.21 | 150 | 38.44 | 150 | 63.70 |
| 6 | 43.47 | 180 | 61.74 | 180 | 63.75 |
| 7 | 43.59 | 210 | 61.82 | | |
| 8 | 43.61 | 240 | 61.91 | | |

Table 2
XPS analysis and KJELDAHL method of different synthesized nanofiber

| XPS analysis | | | | | | | KJELDAHL method |
|---|---|---|---|---|---|---|---|
| Nanofiber | C | O | N | C/O | C/N | O/N | N |
| PAN | 75.89 | 4.90 | 19.21 | 15.49 | 3.951 | 0.255 | 31.25 |
| FPAN1 | 74.72 | 1.40 | 23.88 | 53.37 | 3.12 | 0.058 | 34.52 |
| FPAN2 | 63.55 | 1.10 | 35.35 | 57.77 | 1.798 | 0.031 | 40.28 |
| FPAN3 | 54.00 | 0.80 | 45.20 | 67.50 | 1.195 | 0.018 | 41.88 |

#### 3.5.2. The Effect of pH

The effect of pH on the adsorption of DR80 and DB23 onto various FPAN nanofibers is shown in Fig. 7. For both dyes, the adsorption capacity increased when the pH was decreased. Maximum adsorption of anionic dyes occurred at acidic pH. At lower pHs, more protons will be available to protonate amino groups of FPAN nanofibers to form $NH_3^+$ groups, thereby increasing the electrostatic attractions between negatively charged dye anions and positively charged adsorption sites occurred. As a result, an enhancement is observed in the dye adsorption [29]. When the pH of the solution is raised, a negatively charged site on the adsorbent is generated which is not favorable for the adsorption of anionic dyes because of the electrostatic repulsion [30]. Lower adsorption of DR80 and DB23 dyes at alkaline pH can also be due to the presence of excess $OH^-$ ions competing with the dye anions for the adsorption sites.

#### 3.5.3. The effect of initial dye concentration

The influence of variation of the initial dye concentration on adsorption efficiencies onto various FPAN nanofibers was assessed and the results are shown in Fig. 8. It is clear that the higher the initial dye concentration is, the lower the percentage of dye will be observed. The amount of the adsorbed dye onto the adsorbent raises with an increase in the initial dye concentration. This can be due to the increase in the driving force of the concentration gradient at the higher initial dye concentration (if the amount of adsorbent is kept constant). It can be further stated that repulsion phenomenon occurs between adsorbed dye molecules on one hand, and dye molecules in the aqueous solution on the other hand resultsin a decrease in removal percentage of dye from solution.

It should be noted that in the case of lower concentrations, the ratio of initial number of dye molecules to the available adsorption sites is low, and subsequently, the fractional adsorption becomes independent of initial concentration [31–33].

#### 3.5.4. Adsorption isotherms

The adsorption isotherms investigate the relationship between the mass of the dye adsorbed onto the adsorbent and liquid phase of the dye concentration [34,35]. Various mathematical models can be used to analyze adsorption data. The most common ones include Langmuir, Freundlich, and the Tempkin models [36,37]. The Langmuir isotherm which has successfully been applied to many sorption processes [38–40] can be used to explain the sorption of dye onto various FPAN nanofibers. A basic assumption of the Langmuir theory is that sorption takes place at specific sites within the adsorbent [41,42].

The Langmuir equation can be written as follows [43,44]:

$$q_e = \frac{Q_0 K_L C_e}{1 + K_L C_e} \tag{4}$$

where $q_e$ is the amount of dye adsorbed on the adsorbent at equilibrium (mg/g), $C_e$ denotes the equilibrium concentration of dye solution (mg/L), $K_L$ is the equilibrium constant (L/g), and $Q_0$ is the maximum adsorption capacity (mg/g).

The linear form of Langmuir equation is:

$$\frac{C_e}{q_e} = \frac{1}{K_L Q_0} + \frac{C_e}{Q_0} \tag{5}$$

The isotherm data were also studied by the Freundlich isotherm, which can be expressed by the following equation:

$$q_e = K_F C_e^{\frac{1}{n}} \tag{6}$$

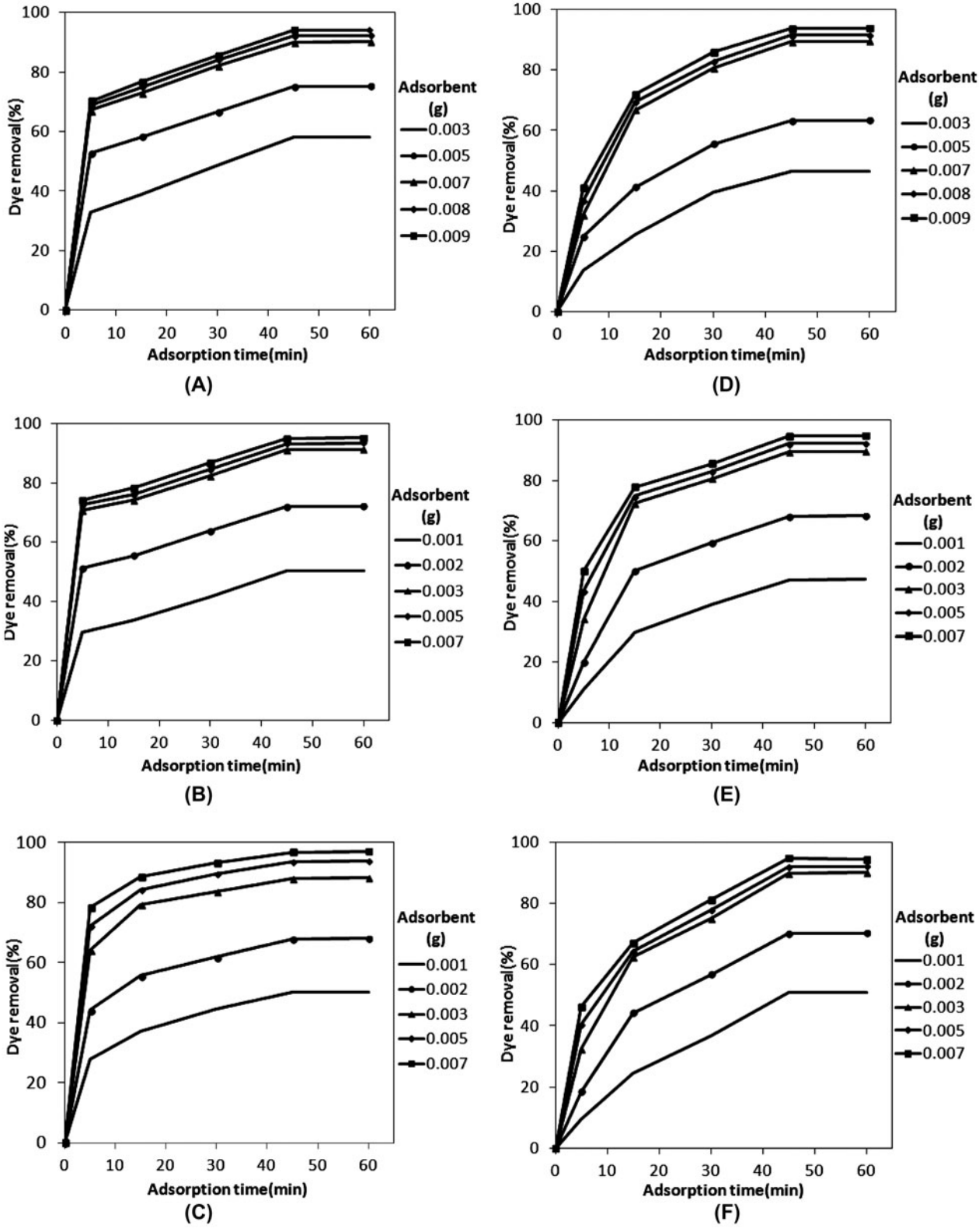


Fig. 6. Effect of adsorbent dosage on the dye removal in different times, (A) FPAN1, $V$ = 30 mL, (B) FPAN2, $V$ = 70 mL, (C) FPAN3, $V$ = 250 mL for DR80, (D) FPAN1, $V$ = 30 mL, (E) FPAN2, $V$ = 70 mL, and (F) FPAN3, $V$ = 250 mL for DR23.

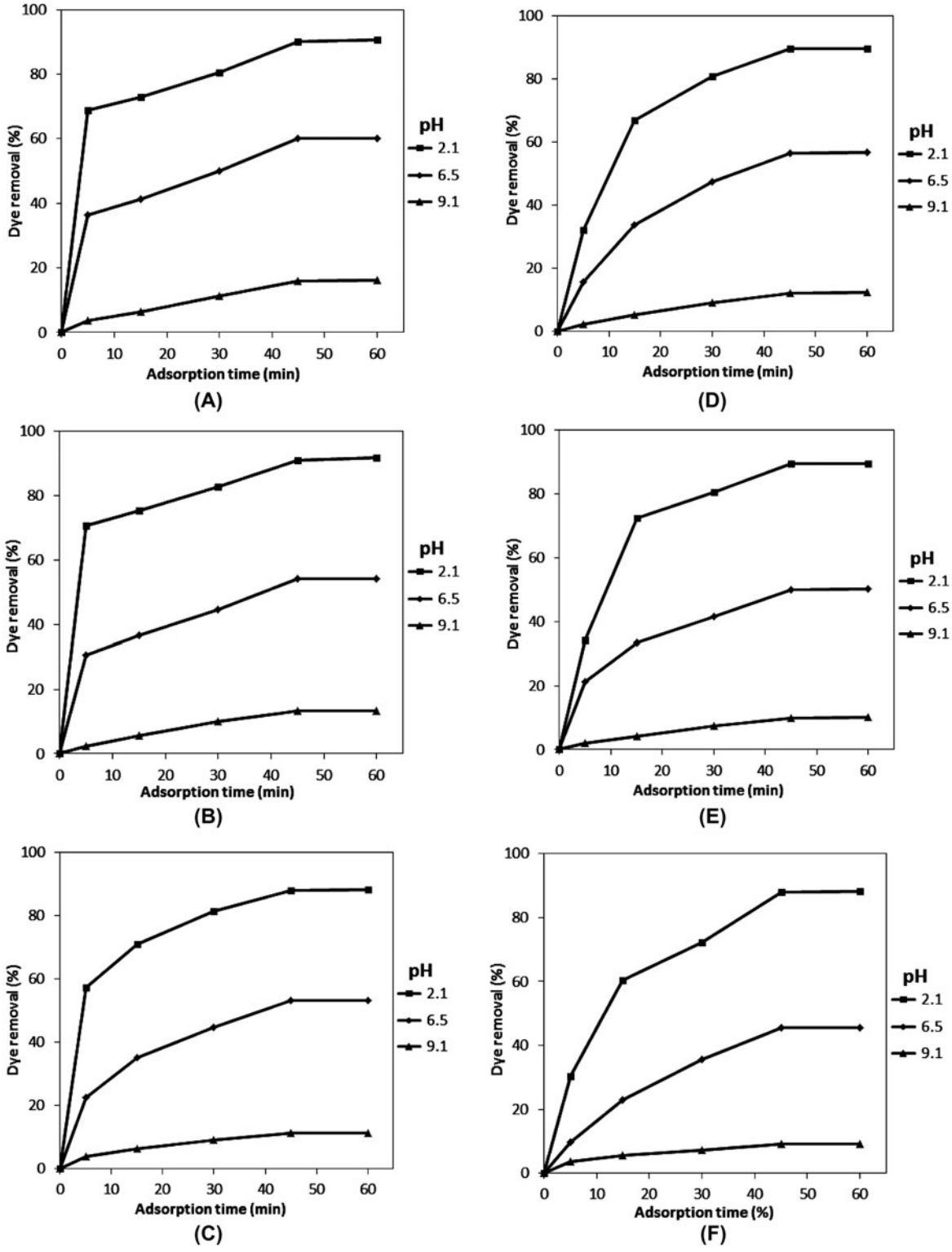


Fig. 7. Effect of the pH on dye removal ability of nanofibers in different times, (A) FPAN1, $V = 30$ mL, (B) FPAN2, $V = 70$ mL, (C) FPAN3, $V = 250$ mL for DR80, (D) FPAN1, $V = 30$ mL, (E) FPAN2, $V = 70$ mL, and (F) FPAN3, $V = 250$ mL for DR23.

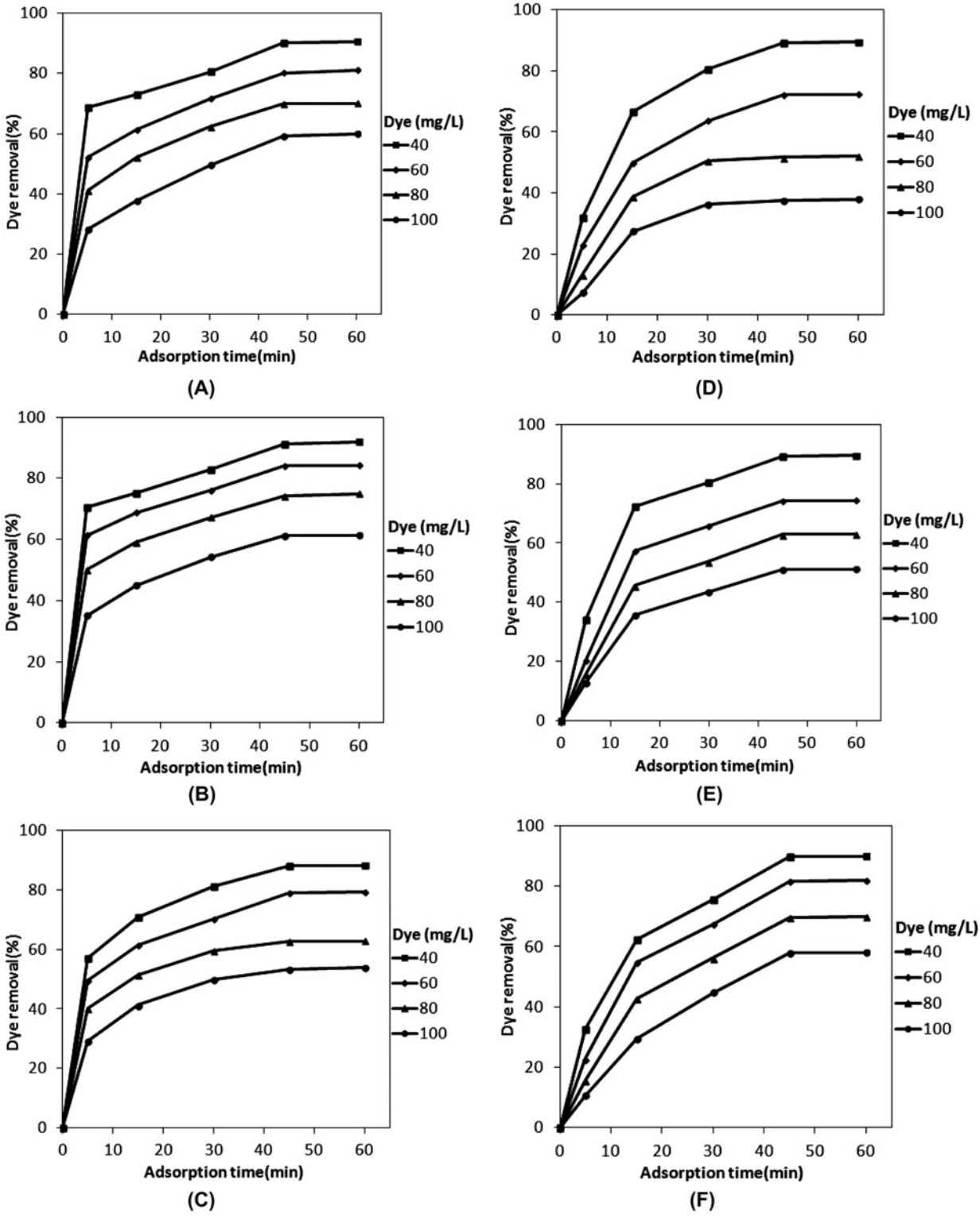


Fig. 8. Effect of the dye concentration on dye removal ability of nanofibers in different times, (A) FPAN1, $V$ = 30 mL, (B) FPAN2, $V$ = 70 mL, (C) FPAN3, $V$ = 250 mL for DR80, (D) FPAN1, $V$ = 30 mL, (E) FPAN2, $V$ = 70 mL, and (F) FPAN3, $V$ = 250 mL for DR23.

where $K_F$ is the adsorption capacity at unit concentration and $\frac{1}{n}$ denotes the adsorption intensity. The $\frac{1}{n}$ values indicate the type of isotherm to be irreversible $\left(\frac{1}{n}=0\right)$, favorable $(0$ , and unfavorable $\left(\frac{1}{n}>\right)$. Eq. (5) can be rearranged to a linear form:

$$\log q_e = \log K_F + \frac{1}{n}\log C_e \tag{7}$$

The basic assumption of this model is that there is an exponential variation in site energies of adsorbent, and also surface adsorption is not a rate limiting step [45]. The Freundlich isotherm is derived by assuming a heterogeneous surface with a nonuniform distribution of heat of adsorption over the surface.

The Tempkin isotherm is given as:

$$q_e = \frac{RT}{b\ \ln(K_T C_e)} \tag{8}$$

Linearized form of Eq. (7) is written as:

$$q_e = B_1 \ln\ K_T + B_1 \ln\ C_e \tag{9}$$

where

$$B_1 = \frac{RT}{b} \tag{10}$$

$K_T$ is the equilibrium binding constant (L/mol) corresponding to the maximum binding energy and constant $B_1$ is related to the heat of adsorption. Also, $T$ is the absolute temperature (K), and $R$ is the universal gas constant (8.314 J mol$^{-1}$ K$^{-1}$).

The basic assumption of this model is that the heat of adsorption of all the molecules in the adsorbed layer decreases linearly with coverage due to adsorbent—adsorbate interactions. Furthermore, the adsorption is characterized by a uniform distribution of binding energies up to some maximum binding energy [46,47].

In this study, in order to determine the constants in Langmuir, Freundlich, and Tempkin isotherms, plots of $C_e/q_e$ versus $C_e$, $\log q_e$ versus $\log C_e$, and $q_e$ versus $\ln C_e$ were drawn, respectively. The coefficient values for various isotherms are shown in Table 3.

As it can be seen from the $R^2$ values of DR80 and DR23, the dye removal isotherm does not follow the Freundlich and Tempkin isotherms. The linear fit between the $C_e/q_e$ versus $C_e$ and $R^2$ values for Langmuir isotherm model showed that the dye removal isotherm can be approximated as Langmuir model (Table 2). This result confirms that the one layer adsorption of DR80 and DR23 takes place at specific homogeneous sites of nanofiber surfaces.

### 3.5.5. Adsorption kinetics

Investigation of the adsorption mechanism onto adsorbents was carried out by characteristic constants of adsorption using pseudo-first-order equation [48], pseudo-second-order equation [49], and intraparticle diffusion [50,51]. A linear form of pseudo-first-order model is:

$$\log(q_e - q_t) = \log(q_e) - \frac{K_1}{2.303}t \tag{11}$$

where $q_e$ is the amount of dye adsorbed at equilibrium (mg/g), $q_t$ denotes the amount of dye adsorbed at the time $t$ (mg/g), and $K_1$ shows the equilibrium rate constant of pseudo-first-order adsorption (min$^{-1}$).

The pseudo-second-order adsorption model, in its final form, can be expressed as follows [52]:

$$\frac{t}{q_t} = \frac{1}{Kq_e^2} + \frac{1}{q_e}t \tag{12}$$

In Eq. (11), $q_e$ is the amount of dye adsorbed at equilibrium (mg/g) and $K_2$ is the pseudo-second-order equilibrium rate constant (g/mg min).

The possibility of intra-particle diffusion resistance affecting adsorption was explored using the intra-particle diffusion model as:

$$q_t = k_p t^{\frac{1}{2}} + I \tag{13}$$

where $k_p$ and $I$ are the intra particle diffusion rate constant and intercept, respectively.

The applicability of the various kinetic models pseudo-first-order, pseudo-second-order, and intra-particle diffusion models for the adsorption of DR80 and BR23 onto adsorbent at different dye concentrations. Linear plots of $\log(q_e - q_t)$ versus contact time $(t)$, $t/q_t$ versus contact time $(t)$ and $q_t$ against $t^{1/2}$ are presented. The values of $k_1$, $k_2$, $k_p$, $I$, $R^2$, and the calculated $q_e((q_e)_{Cal.})$ are given in Table 4.

Results illustrated that the rates of sorption conform to the pseudo-second-order kinetic model with good coefficients of determination. In addition, the experimental $q_e((q_e)_{Exp.})$ values are in accordance with the calculated ones $((q_e)_{Cal.})$ obtained from the linear plots of pseudo-second-order kinetics.

Table 3
Linearized isotherm coefficients for dye adsorption at different dye concentration

| | | Langmuir | | | | Freundlich | | | Tempkin | |
|---|---|---|---|---|---|---|---|---|---|---|
| Adsorbent | Dye | $Q_0$ | $K_L$ | $R^2$ | $1/n$ | $K_F$ | $R^2$ | $K_T$ | $B_1$ | $R^2$ |
| FPAN1 | DR80 | 277.77 | 0.300 | 0.999 | 0.215 | 117.48 | 0.981 | 9.80 | 43.41 | 0.983 |
| | DR23 | 163.93 | 0.782 | 0.995 | 0.029 | 151.35 | 0.164 | 1,940.82 | 4.70 | 0.141 |
| FPAN2 | DR80 | 2,500 | 0.363 | 0.999 | 0.213 | 1,045.2 | 0.935 | 12.45 | 361.43 | 0.952 |
| | DR23 | 1,250 | 0.400 | 0.999 | 0.155 | 660.69 | 0.975 | 54.47 | 154.56 | 0.978 |
| FPAN3 | DR80 | 5,000 | 0.333 | 0.998 | 0.176 | 2,290.8 | 0.908 | 24.53 | 644.57 | 0.931 |
| | DR23 | 5,000 | 0.4 | 1 | 0.204 | 2,344.22 | 0.933 | 12.70 | 793.12 | 0.959 |

Table 4
Kinetic constants for dye adsorption on the surface-modified PAN nanofibers at different dye concentration

| | | | Pseudo-first order | | | Pseudo-second order | | | Intraparticle diffusion | | |
|---|---|---|---|---|---|---|---|---|---|---|---|
| Adsorbent | Dye (mg/L) | $(q_e)_{Exp.}$ | $R^2$ | $(q_e)_{Cal.}$ | $K_1$ | $R^2$ | $(q_e)_{Cal.}$ | $K_2$ | $R^2$ | $I$ | $k_p$ |
| FPAN1 | *DR80* | | | | | | | | | | |
| | 40 | 155.28 | 0.848 | 127.05 | 0.097 | 0.959 | 138.88 | 0.0031 | 0.780 | 37.23 | 17.69 |
| | 60 | 208.33 | 0.926 | 181.97 | 0.090 | 0.967 | 188.67 | 0.0242 | 0.863 | 39.57 | 28.06 |
| | 80 | 240.37 | 0.899 | 309.74 | 0.138 | 0.979 | 222.22 | 0.0465 | 0.882 | 41.84 | 29.92 |
| | 100 | 256.62 | 0.913 | 285.75 | 0.087 | 0.955 | 256.41 | 0.0680 | 0.916 | 24.16 | 33.01 |
| | *DR23* | | | | | | | | | | |
| | 40 | 153.42 | 0.939 | 210.86 | 0.103 | 0.992 | 153.84 | 0.0011 | 0.938 | 12.16 | 20.80 |
| | 60 | 185.73 | 0.930 | 158.48 | 0.053 | 0.991 | 188.67 | 0.0051 | 0.934 | 11.64 | 24.81 |
| | 80 | 178.28 | 0.862 | 158.96 | 0.098 | 0.984 | 192.30 | 0.0078 | 0.913 | 7.76 | 25.39 |
| | 100 | 176.57 | 0.929 | 224.90 | 0.104 | 0.910 | 185.18 | 0.0095 | 0.940 | 3.24 | 25.91 |
| FPAN2 | *DR80* | | | | | | | | | | |
| | 40 | 1,287.72 | 0.894 | 903.64 | 0.087 | 0.968 | 1,111.11 | 0.0050 | 0.768 | 322.12 | 146.56 |
| | 60 | 1,766.94 | 0.839 | 1,698.24 | 0.121 | 0.959 | 1,666.66 | 0.0043 | 0.793 | 416.51 | 204.33 |
| | 80 | 2,099.72 | 0.936 | 1,659.58 | 0.087 | 0.970 | 2,000 | 0.0059 | 0.839 | 434.96 | 249.56 |
| | 100 | 2,144.80 | 0.953 | 2,401.59 | 0.124 | 0.983 | 2,000 | 0.0101 | 0.886 | 361.42 | 269.56 |
| | *DR23* | | | | | | | | | | |
| | 40 | 835.33 | 0.860 | 794.32 | 0.124 | 0.989 | 833.33 | 0.0095 | 0.764 | 197.51 | 97 |
| | 60 | 1,040.62 | 0.880 | 1,659.58 | 0.138 | 0.989 | 1,111.11 | 0.011 | 0.925 | 52.46 | 144.91 |
| | 80 | 1,175.44 | 0.862 | 1,967.88 | 0.133 | 0.991 | 1,250 | 0.017 | 0.942 | 36.20 | 164.55 |
| | 100 | 1,194.66 | 0.857 | 2,073 | 0.134 | 0.988 | 1,250 | 0.021 | 0.951 | 28.71 | 167.60 |
| FPAN3 | *DR80* | | | | | | | | | | |
| | 40 | 2,996.66 | 0.969 | 1,995.28 | 0.116 | 0.982 | 2,857.14 | 0.00004 | 0.743 | 805.18 | 344.72 |
| | 60 | 3,927.51 | 0.929 | 3,019.95 | 0.105 | 0.946 | 4,000 | 0.00045 | 0.774 | 979.45 | 453.89 |
| | 80 | 4,189.33 | 0.915 | 2,754.22 | 0.098 | 0.975 | 4,058.57 | 0.00045 | 0.740 | 1,128.7 | 475.46 |
| | 100 | 4,240.80 | 0.954 | 2,511.88 | 0.093 | 0.980 | 4,249.21 | 0.00047 | 0.742 | 1,141 | 484.94 |
| | *DR23* | | | | | | | | | | |
| | 40 | 3,000 | 0.912 | 3,564.51 | 0.093 | 0.974 | 3,030.03 | 0.0099 | 0.948 | 202.01 | 393.97 |
| | 60 | 4,094 | 0.833 | 6,918.30 | 0.129 | 0.981 | 4,000 | 0.0171 | 0.957 | 79.50 | 576.31 |
| | 80 | 4,650 | 0.817 | 8,317.63 | 0.125 | 0.975 | 4,545.45 | 0.0209 | 0.959 | 9.27 | 665.87 |
| | 100 | 4,511.27 | 0.894 | 7,014.55 | 0.103 | 0.992 | 4,524.88 | 0.0271 | 0.957 | 2.19 | 667.95 |

## 4. Conclusion

In this paper, amine-containing compounds including DEA, DETA, and TETA were used for grafting to polyacrylonitrile (PAN) nanofibers and their dye removal abilities were investigated. Direct red 80 (DR80) and Direct red 23 (DR23) were used as model compounds. It was estimated that the required time for the functionalization process increased by 1 h with every 10°C decrease in boiling point of an amine-containing compound compared to the chosen reaction

temperature (95˚C). The results indicated that a chemical reaction occurred between nitrile groups of PAN nanofibers and amine groups of DEA, DETA, and TETA, affecting the chemical characteristics of nanofibers. The results also showed some defects, cracks, and signs of degradation on the surface of the FPAN (functionalized PAN) nanofiber for FPAN1 (with diethylamine compound) and conglutination to each other at touching points and becoming intertwined due to crosslinking role of the amine compound for FPAN3 (with triethylenetetramine) nanofiber. The AFM result demonstrated that the surfaces of the PAN nanofiber became rough after the functionalization of the PAN nanofiber and the average roughness value for FPAN1 was higher than that of FPAN2. Also, the highest value of $S_a$ was for FPAN3. We found that adsorption of DR80 and DR23 by different FPAN nanofibers follows the Langmuir isotherm. The adsorption kinetic of dyes was found to conform to pseudo-second-order kinetics. Here, we stated that FPAN nanofibers produced by various amine-containing compounds are suitable alternatives to many other adsorbents for anionic dye removal from colored aqueous solutions.

## References


[1] N.M. Mahmoodi, Equilibrium, kinetic and thermodynamic of dye removal using alginate from binary system, J. Chem. Eng. Data 56 (2011) 2802–2811.

[2] K. Nuithitikul, S. Srikhun, S. Hirunpraditkoon, Kinetics and equilibrium adsorption of basic green 4 dye on activated carbon derived from durian peel: Effects of pyrolysis and post-treatment conditions, J. Taiwan Inst. Chem. Eng. 41 (2010) 591–598.

[3] M. Ghaedi, M. Pakniat, Z. Mahmoudi, S. Hajati, R. Sahraei, A. Daneshfar, Synthesis of nickel sulfide nanoparticles loaded on activated carbon as a novel adsorbent for the competitive removal of Methylene blue and Safranin-O, Spectrochim. Acta, Part A 123 (2014) 402–409.

[4] B.-Y. Chen, M.-M. Zhang, Y. Ding, C.-T. Chang, Feasibility study of simultaneous bioelectricity generation and dye decolorization using naturally occurring decolorizers, J. Taiwan Inst. Chem. Eng. 41 (2010) 682–688.

[5] N.M. Mahmoodi, Photocatalytic ozonation of dyes using copper ferrite nanoparticle prepared by co-precipitation method, Desalination 279 (2011) 332–337.

[6] R.G. Saratale, G.D. Saratale, J.S. Chang, S.P. Govindwar, Bacterial decolorization and degradation of azo dyes: A review, J. Taiwan Inst. Chem. Eng. 42 (2011) 138–157.

[7] Y. He, G.-M. Li, H. Wang, Z.-W. Jiang, J.-F. Zhao, H.-X. Su, Experimental study on the rejection of salt and dye with cellulose acetate nanofiltration membrane, J. Taiwan Inst. Chem. Eng. 40 (2009) 289–295.

[8] Q. Qin, J. Ma, K. Liu, Adsorption of anionic dyes on ammonium-functionalized MCM-41, J. Hazard. Mater. 162 (2009) 133–139.

[9] C. Namasivayam, R. Radhika, S. Suba, Uptake of dyes by a promising locally available agricultural solid waste: Coir pith, Waste Manage. 21 (2001) 381–387.

[10] H. Yang, Q. Feng, Characterization of pore-expanded amino-functionalized mesoporous silicas directly synthesized with dimethyldecylamine and its application for decolorization of sulphonated azo dyes, J. Hazard. Mater. 180 (2010) 106–114.

[11] H. Yang, Q. Feng, Direct synthesis of pore-expanded amino-functionalized mesoporous silicas with dimethyldecylamine and the effect of expander dosage on their characterization and decolorization of sulphonated azo dyes, Micropor. Mesopor. Mater. 135 (2010) 124–130.

[12] L. Chaoa, L. Zhaoyang, L. Aimin, L. Wei, J. Zhenmao, Ch. Jinlong, Zh. Quanxing, Adsorption of reactive dyes onto polymeric adsorbents: effect of pore structure and surface chemistry group of adsorbent on adsorptive properties, Sep. Purif. Technol. 44 (2005) 91–96.

[13] M. Machida, B. Fotoohi, Y. Amamo, T. Ohba, H. Kanoh, L. Mercier, Cadmium(II) adsorption using functional mesoporous silica and activated carbon, J. Hazard. Mater. 221–222 (2012) 220–227.

[14] N.M. Mahmoodi, Synthesis of amine-functionalized magnetic ferrite nanoparticle and its dye removal ability, J. Environ. Eng. 139 (2013) 1382–1390.

[15] M. Shaiful Sajab, Ch. Hua Chia, S. Zakaria, S. Mohd Jani, M. Khan Ayob, K. Leong Chee, P. Sim Khiew, W. Siong Chiu, Citric acid modified kenaf core fibres for removal of methylene blue from aqueous solution, Bioresour. Technol. 102 (2011) 7237–7243.

[16] T.S. Anirudhan, P.S. Suchithra, S. Rijith, Amine-modified polyacrylamide–bentonite composite for the adsorption of humic acid in aqueous solutions, Colloids Surf., A 326 (2008) 147–156.

[17] A.M. Shoushtari, M. Zargaran, M. Abdouss, Preparation and characterization of high efficiency ion-exchange crosslinked acrylic fibers, J. Appl. Polym. Sci. 101 (2006) 2202–2209.

[18] P. Tahaei, M. Abdouss, M. Edrissi, A.M. Shoushtari, M. Zargaran, Preparation of chelating fibrous polymer by different diamines and study on their physical and chemical properties, Materialwissenschaft und Werkstofftechnik 39 (2008) 839–844.

[19] M. Avila, T. Burks, F. Akhtar, M. Göthelid, P.C. Lansåker, M.S. Toprak, M. Muhammed, A. Uheida, Surface functionalized nanofibers for the removal of chromium(VI) from aqueous solutions, Chem. Eng. J. 245 (2014) 201–209.

[20] W. Jianqiang, K. Pan, H. Qiwei, C. Bing, Polyacrylonitrile/polypyrrole core/shell nanofiber mat for the removal of hexavalent chromium from aqueous solution, J. Hazard. Mater. 244–245 (2013) 121–129.

[21] Z. Chen, X. Feng, D. Han, L. Wang, W. Cao, L. Shao, Preparation of aminated polyacrylonitrile porous fiber mat and its application for Cr(VI) ion removal, Fibers Polym. 15 (2014) 1364–1368.

[22] K. Saeed, S. Haider, T.J. Oh, S.Y.J. Park, Preparation of amidoxime-modified polyacrylonitrile (PAN-oxime)

nanofibers and their applications to metal ions adsorption, J. Membr. Sci. 322 (2008) 400–405.
[23] P. Kampalanonwat, P. Supaphol, Preparation and adsorption behavior of aminated electrospun polyacrylonitrile nanofiber mats for heavy metal ion removal, Am. Chem. Soc. 12 (2010) 3619–3627.
[24] B. Bagheri1, M. Abdouss, M. Mohammadi Aslzadeh, A. Mousavi Shoushtari, Efficient removal of $Cr^{3+}$, $Pb^{2+}$ and $Hg^{2+}$ ions from industrial effluents by hydrolyzed/thioamidated polyacrylonitrile fibres, Iran. Polym. J. 19 (2010) 911–925.
[25] M. Parvinzadeh, S. Moradian, A. Rashidi, M.E. Yazdanshenas, Effect of the addition of modified nanoclays on the surface properties of the resultant polyethylene terephthalate/clay nanocomposites, Polym.-Plast. Technol. Eng 49 (2010) 1–11.
[26] P. Karimi Neghlani, M. Rafizadeh, F. Afshar Taromi, Preparation of aminated-polyacrylonitrile nanofiber membranes for the adsorption of metal ions: Comparison with microfibers, J. Hazard. Mater. 186 (2011) 182–189.
[27] A.I. Vogel, Elementary Practical Organic Chemistry Part III Quantitative Organic Analysis, D.Sc, Woolwich Polytechnic, Beit Scientific Research Fellow of the Imperial College, London, 1958, pp. 658–665
[28] G. Crini, F. Gimbert, C. Robert, B. Martel, O. Adam, N. Morin-Crini, The removal of basic Blue 3 from aqueous solutions by chitosan-based adsorbent: Batch studies, J. Hazard. Mater. 153 (2008) 96–106.
[29] N.M. Mahmoodi, Sh. Khorramfar, F. Najafi, Amine-functionalized silica nanoparticle: Preparation, characterization and anionic dye removal ability, Desalination 279 (2011) 61–68.
[30] N.M. Mahmoodi, A. Maghsoudi, F. Najafi, M. Jalili, H. Kharrati, Primary–secondary amino silica nanoparticle: synthesis and dye removal from binary system, Desalin. Water Treat. 279(1–3) (2011) 61–68.
[31] S. Chatterjee, S. Chatterjee, B.P. Chatterjee, A.R. Das, A.K. Guha, Adsorption of a model anionic dye, eosin Y, from aqueous solution by chitosan hydrobeads, J. Colloid Interface Sci. 288 (2005) 30–35.
[32] G. Crini, P.M. Badot, Application of chitosan, a natural aminopolysaccharide, for dye removal from aqueous solutions by adsorption processes using batch studies: A review of recent literature, Prog. Polym. Sci. 33 (2008) 399–447.
[33] N.M. Mahmoodi, J. Abdi, F. Najafi, Gemini polymeric nanoarchitecture as a novel adsorbent: Synthesis and dye removal from multicomponent system, J. Colloid Interface Sci. 400 (2013) 88–96.
[34] M. Uğurlu, Adsorption of a textile dye onto activated sepiolite, Micropor. Mesopor. Mater. 119 (2009) 276–283.
[35] N.M. Mahmoodi, Nickel ferrite nanoparticle: Synthesis, modification by surfactant and dye removal ability, Water, Air, Soil Pollut. 224 (2013) 1419–1429.
[36] W. Shen, S. Chen, S. Shi, X. Li, X. Zhang, W. Hu, H. Wang, Adsorption of Cu(II) and Pb(II) onto diethylenetriamine-bacterial cellulose, Carbohyd. Polym. 75 (2009) 110–114.
[37] M.V. Dinu, E.S. Dragan, Heavy metals adsorption on some iminodiacetate chelating resins as a function of the adsorption parameters, React. Funct. Polym. 68 (2008) 1346–1354.
[38] X. Zhang, Sh. Zheng, Zh. Lin, J. Zhang, Removal of basic fuchsin dye by adsorption onto polyacrylamide/laponite nanocomposite hydrogels 42 (2012) 1273–1277.
[39] W. Yongsheng, Z. Li, R. Xuefeng, S. Hai, W. Aiqin, Removal of methyl violet from aqueous solutions using poly (acrylic acid-co-acrylamide)/attapulgite composite, J. Environ. Sci. 22 (2010) 7–14.
[40] Z. Tang, J. Wu, Q. Li, Z. Lan, L. Fan, J. Lin, M. Huang, The preparation of poly(glycidyl acrylate)–polypyrrole gel-electrolyte and its application in dye-sensitized solar cells, Electrochim. Acta 55 (2010) 4883.
[41] I. Langmuir, The constitution and fundamental properties of solids and liquids. PART I. Solids, J. Am. Chem. Soc. 38 (1916) 2221–2295.
[42] I. Langmuir, The constitution and fundamental properties of solids and liquids. II. Liquids. 1, J. Am. Chem. Soc. 39 (1917) 1848–1906.
[43] A. Dastbaz, A.R. Keshtkar, Adsorption of $Th^{4+}$, $U^{6+}$, $Cd^{2+}$, and $Ni^{2+}$ from aqueous solution by a novel modified polyacrylonitrile composite nanofiber adsorbent prepared by electrospinning, Appl. Surf. Sci. 293 (2014) 336–344.
[44] L.D. Benefield, J.F. Judkins, B.L. Weand, Process Chemistry for Water and Wastewater Treatment, Prentice-Hall, Inc., Englewood Cliffs, NJ, 1982, pp. 191–210.
[45] M.R. Fathi, A. Asfaram, A. Farhangi, Removal of Direct red 23 from aqueous solution using corn stalks: Isotherms, kinetics and thermodynamic studies, Spectrochim. Acta, Part A 135 (2015) 364–372.
[46] M.J. Tempkin, V. Pyzhev, Recent modification to Langmiur isotherms, Acta Physiochim. USSR 12 (1940) 217–222.
[47] Y.C. Kim, C. Kim, I. Choi, S. Rengaraj, Arsenic removal using mesoporous alumina prepared via a templating method, Environ. Sci. Technol. 38 (2004) 924–931.
[48] N.M. Mahmoodi, Magnetic ferrite nanoparticle–alginate composite: Synthesis, characterization and binary system dye removal, J. Taiwan Inst. Chem. Eng. 44 (2013) 322–330.
[49] N.M. Mahmoodi, U. Sadeghi, A. Maleki, B. Hayati, F. Najafi, Synthesis of cationic polymeric adsorbent and dye removal isotherm, kinetic and thermodynamic, J. Ind. Eng. Chem. 20 (2014) 2745–2753.
[50] A. Özcan, A.S. Özcan, Adsorption of acid red 57 from aqueous solutions onto surfactant-modified sepiolite, J. Hazard. Mater. 125 (2005) 252–259.
[51] S. Kaur, S. Rani, R. Kumar Mahajan, Adsorption of dye crystal violet onto surface-modified *Eichhornia crassipes*, Desalin. Water Treat. 53(7) (2013) 1–13.
[52] M. Monier, D.M. Ayad, A.A. Sarhan, Adsorption of Cu(II), Co(II), and Ni(II) ions by modified magnetic chitosan chelating resin, J. Hazard. Mater. 176 (2009) 348–355.